

AD-A111 486

NAVAL RESEARCH LAB WASHINGTON DC

F/8 4/1

THE S3-S IONOSPHERIC IRREGULARITIES SATELLITE EXPERIMENT: PROBE--ETC(U)

FEB 82 E P SZUSZCZEWICZ, J C HOLMES, M SINGH

UNCLASSIFIED

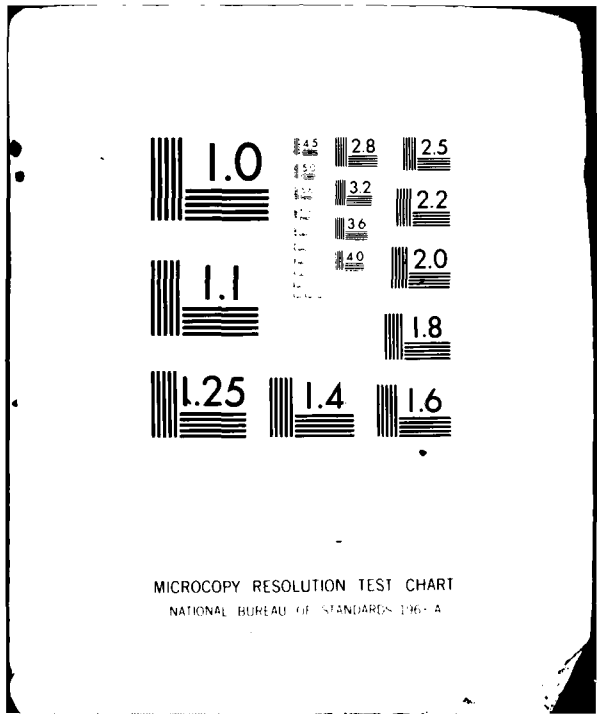
NRL-NR-4728

NL

101
102



END
DATE
FILMED
82
DTIC



MICROCOPY RESOLUTION TEST CHART
NATIONAL BUREAU OF STANDARDS-1963-A

AD A 111 456

SECURITY CLASSIFICATION OF THIS PAGE (When Data Entered)

REPORT DOCUMENTATION PAGE		READ INSTRUCTIONS BEFORE COMPLETING FORM
1. REPORT NUMBER NRL Memorandum Report 4728	2. GOVT ACCESSION NO. AD-A112456	3. RECIPIENT'S CATALOG NUMBER
4. TITLE (and Subtitle) THE S3-4 IONOSPHERIC IRREGULARITIES SATELLITE EXPERIMENT: PROBE DETECTION OF MULTI-ION COMPO- NENT PLASMAS AND ASSOCIATED EFFECTS ON INSTA- BILITY PROCESSES	5. TYPE OF REPORT & PERIOD COVERED Interim report on a continuing NRL problem.	
	6. PERFORMING ORG. REPORT NUMBER	
7. AUTHOR(s) E. P. Szuszczewicz, J. C. Holmes, and M Singh*	8. CONTRACT OR GRANT NUMBER(s)	
9. PERFORMING ORGANIZATION NAME AND ADDRESS Naval Research Laboratory Washington, DC 20375	10. PROGRAM ELEMENT, PROJECT, TASK AREA & WORK UNIT NUMBERS 61153N; RR033-02-44; 41-0949-0-2	
11. CONTROLLING OFFICE NAME AND ADDRESS Office of Naval Research Arlington, VA 22217	12. REPORT DATE February 11, 1982	
	13. NUMBER OF PAGES 30	
14. MONITORING AGENCY NAME & ADDRESS (if different from Controlling Office)	15. SECURITY CLASS. (of this report) UNCLASSIFIED	
	15a. DECLASSIFICATION/DOWNGRADING SCHEDULE	
16. DISTRIBUTION STATEMENT (of this Report) Approved for public release; distribution unlimited.		
17. DISTRIBUTION STATEMENT (of the abstract entered in Block 20, if different from Report)		
18. SUPPLEMENTARY NOTES *Present address: Sachs/Freeman Associates, Inc., Bowie, MD 20715. On leave from Punjabi University, Patiala, India.		
19. KEY WORDS (Continue on reverse side if necessary and identify by block number) Ionospheric irregularities Power spectrum Satellite measurements Plasma diagnostics		
20. ABSTRACT (Continue on reverse side if necessary and identify by block number) The pulsed plasma probe technique has been expanded to include simultaneous determinations of absolute electron density, density fluctuations, electron temperature, and mean ion mass with resolution limited only by probe geometry, sheath size, and telemetry. The technique has been designed to test for coupling of electron density variations and ion composition irregularities in multi-component plasmas by the comparison of electron density fluctuation power spectra $P_N(k)$ and a newly developed diagnostic parameter, the mean ion mass fluctuation spectra $\delta\bar{M}_i/\bar{M}_i - P_M(k)$. In addition, the experiment		

DD FORM 1473
1 JAN 73

EDITION OF 1 NOV 65 IS OBSOLETE
S/N 0102-014-6601

SECURITY CLASSIFICATION OF THIS PAGE (When Data Entered)

Set in Mark & Co. / Mark & Co. app. 2-1-82 the limit
of Para 4

20. ABSTRACT (Continued)

extends satellite-borne irregularity spectral analyses down to the 5-20 meter range while attempting to synthesize F-region plasma instability processes on the basis of N_e , T_e , ΔN_e , P_N and P_M . Initial results demonstrate the expanded diagnostic capability for high spatial resolution measurements of mean ion mass and provide experimental evidence for the role of ion composition in multi-stepped plasma instability processes. Specific results include a spectral index X_n in $P_N = A_n f^{-X_n}$ of 1.6-2.9 over the wavelength range from 1 km to 6 meters under conditions identified with an unstable equatorial nighttime ionosphere. Simultaneous measurements of $\delta \bar{M}_i / \bar{M}_i \rightarrow (P_M = A_m f^{-X_m})$ and $\delta N_e / \bar{N}_e \rightarrow (P_N = A_n f^{-X_n})$ have shown a general behavior tending to lower power ($A_m < A_n$) and softer spectra ($X_m < X_n$) in ion mass fluctuations when compared with fluctuations in total plasma density. Limited analyses of the two power spectral elements raises hopes for the differentiation between plasma mechanisms that can lead to similar indices in P_N .

**THE S3-4 IONOSPHERIC IRREGULARITIES SATELLITE EXPERIMENT:
PROBE DETECTION OF MULTI-ION COMPONENT PLASMAS
AND ASSOCIATED EFFECTS ON INSTABILITY PROCESSES**

INTRODUCTION

In recent years interest in ionospheric research has turned from the definition of the zero-order ionosphere to an understanding of the more dynamic processes involving plasma instability mechanisms and their cause-effect relationships. While much progress has been made, more detailed experimental and theoretical work is needed to unfold the active first principles that govern the geoplasma environment. For example, we have yet to define the electron density fluctuation power spectrum over the broad domain encompassed by equatorial spread-F (tens of kilometers to fractions of a meter).

It is noted that density fluctuation power spectra represent an important approach to understanding the multi-stepped plasma processes in which large scale irregularities cascade to much smaller dimensions. In this regard the works of Dyson et al. (1974), along with the cataloging efforts of McClure and Hanson (1973) have identified some characteristic spectral features down to 70 meters. From here the definition of spectral characteristics needs to be extended down to sizes less than 1 meter (e.g., Huba et al. 1978 and associated references), and the same spectral characteristics must be studied within the context of positions relative to the F-layer peak (Ossakow et al, 1979) and any superimposed ionospheric depletions (McClure et al. 1977 and Szuszczewicz, 1978). These measurements must be time correlated in order to study the development of multi-step instability processes.

Extended studies of fluctuation power spectra cannot stand alone in determining all the causal mechanisms. Existing equatorial data show that studies of F-region irregularities must determine the degree of balance between the chemistry and dynamics. To this end, the temperature and high resolution ion composition measurements must be made inside and outside of ionospheric holes, as well as across the sharp boundaries that are a characteristic feature of many of the depleted domains. The temperature measurement should also be done simultaneously with the determination of electron density power spectra in order to determine the role of electron energy in the naturally occurring instability processes (Ossakow, 1974).

In order to develop a more comprehensive experimental profile on ionospheric irregularity structures, the pulsed plasma probe technique (Szuszczewicz and Holmes, 1975) has been expanded to include measurements of electron density fluctuations and variations in mean ion mass. These measurements are conducted simultaneously with the standard determinations of absolute electron density (N_e), temperature (T_e) and plasma potential (V_∞). The capability for high spatial resolution measurements of mean ion mass opens up the possibility of exploring the coupling of electron density variations and ion composition irregularities by the comparison of electron density fluctuation power spectra $P_N(k)$ and a newly developed

parameter, the mean ion mass fluctuation power spectra, $P_M(k)$. The new instrument (designated NRL-747) has been successfully flown on the lower F-region, polar orbiting, sun-synchronous (2230 LT equatorial crossing) STP/S3-4 satellite launched in March 1978. The orbit allows a global study of N_e , T_e and $P_N(k)$, an information set that will help catalogue similarities and differences between polar and equatorial irregularities and ultimately sort out first and second-order cause-effect relationships operating between plasma instabilities and ionospheric irregularities. The experiment provides the first effort to study the role of ion composition in the distribution of wave energy in the cascading process of large-to-small scale ionospheric plasma irregularities, a role considered important at the equator during the occurrence of spread-F conditions and potentially important at high latitudes under conditions of current-convective instability.

Figure 1 schematically depicts the latitudinal differences in the irregular ionosphere at F-region altitudes, with one of the initial investigative targets in the S3-4 effort being the complete experimental definition of thermal electron distributions in the "biteouts" at nighttime equatorial latitudes under spread-F conditions. These "biteouts" are naturally occurring ionospheric holes which can be three decades deep in depletion and can have widths ranging from fractions of a kilometer to tens of kilometers (see e.g., McClure et al., 1973 and 1977; Szuszczewicz, 1978; and

Szuszczewicz et al., 1981). There can be major changes in ion chemistry which take place across the boundaries of the holes...changes which now appear to be trendable and strongly coupled to the mechanism(s) which generate the holes themselves (Szuszczewicz et al., 1980; Narcisi and Szuszczewicz, 1981), and cascade the irregularity distributions from 10's of kilometers to fractions of a meter (e.g., Keskinen et al., 1981; Kelly et al., 1981).

Outside the latitudinal domain of equatorial spread-F, the regions of primary interest in the S3-4 study of F-region irregularities involve the main trough, auroral oval, and domains encompassing the ring current, polar wind and the cusp. The mid-latitude and dayside equatorial F-regions are generally very regular in structure and consequently of less interest.

Within the framework of the relatively simple picture in Figure 1, the improved plasma diagnostic capabilities on the S3-4 satellite and associated analysis efforts will attempt to assemble a relatively comprehensive catalogue of polar and equatorial irregularities along with an improved understanding of their cause-effect relationships. Indeed, some initial efforts have already been published (Singh et al., 1981; Rodriguez et. al., 1981; and Szuszczewicz et al., 1981). In the subsequent sections, the experimental technique will be described, associated data presented, and evidence will be provided which suggests that ion composition plays an important role in multi-stepped plasma instability processes active in the F-region ionosphere.

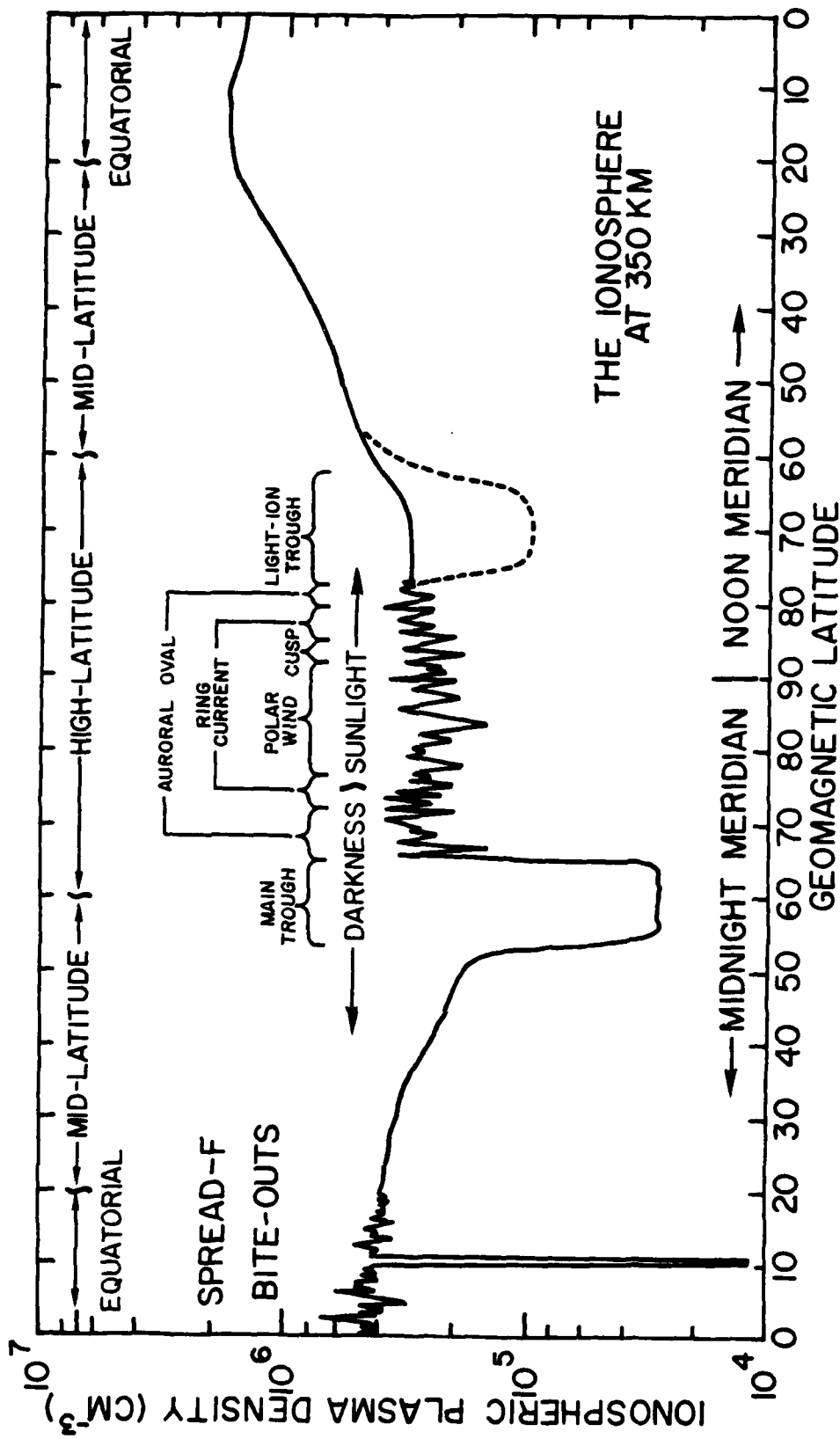


Fig. 1 — Schematic representation of F-region plasma density irregularities and associated geophysical domains

THE EXPERIMENTAL TECHNIQUE

The NRL-747 experiment employs a pair of pulsed plasma probes (P⁴ is the designated acronym), each of which is capable of simultaneous measurement of electron density, temperature and density fluctuation power spectra regardless of the state of turbulence or the degree of irregularity in the ionospheric plasma medium. Together, the pair of probes also provide mean ion mass fluctuation measurements to a maximum Nyquist frequency of 200 Hz. The instrument is a Langmuir-type probe using a special electronic procedure for generating the current-voltage characteristic (Holmes and Szuszczewicz, 1975; Szuszczewicz and Holmes, 1975). The pulse modulated approach reduces the distortion of the current-voltage characteristic that can result from surface contamination and allows millisecond tracking of density fluctuations that might occur during the time required to generate the current voltage characteristic. (The temporal resolution is limited only by telemetry.)

Subject to the selection of 1 of 8 commandable modes of operation, each of the probes had applied to it some variation of the voltage function illustrated in Figure 2. The pulse modulated waveform, following the sawtooth envelope, provides the fundamental data set for a "conventional" Langmuir current-voltage characteristic and associated determinations of N_e and T_e (Chen, 1965) at a nominal 3 Hz rate. During the interpulse period, a fixed-voltage V_B is applied, with

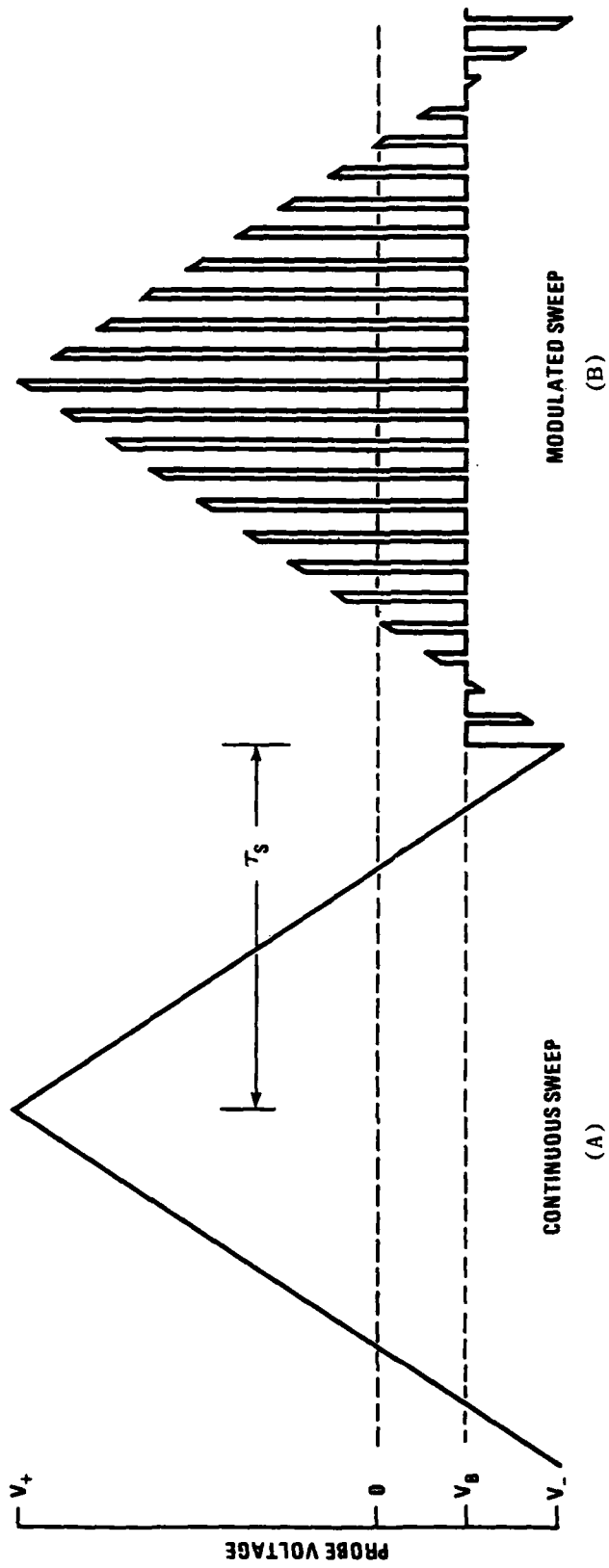


Fig. 2 -- Voltage format utilized in the pulsed-sweep mode of the pulsed-plasma-probe (P^3) technique

associated current measurements providing a running measure of density fluctuations (assuming $\delta I_B \propto \delta N_e$) and a time-dependent data set for power spectral analysis with a Nyquist frequency of 400 Hz in the high data-rate mode. In addition to pulse-modulation, each of the probes could be operated in a simple fixed-bias mode and as a "conventional" continuous-sweep Langmuir probe, the latter having been introduced for systematic studies of hysteresis and contamination effects during satellite mission lifetimes (a minor mission objective).

The probes were routinely operated with V_B on one probe set for electron-saturation-current collection (defined as the E-probe with $I_B = I_e(\text{sat}) \equiv E$) while the value of V_B on the second probe was biased for ion saturation current collection (defined as the I probe with $I_B = I_i(\text{sat}) \equiv I$). The expressions for the currents collected by the two cylindrical probes take the forms

$$E \equiv I_e(\text{sat}) = N_e \sqrt{\frac{kT_e}{2\pi M_e}} A_p e \left\{ \sqrt{\frac{2}{\pi}} \left(1 + \frac{e\phi_p^e}{kT_e} \right)^{\frac{1}{2}} \right\} \quad (1)$$

(Chen, 1965; for thick sheaths) and

$$I \equiv I_i(\text{sat}) = N_i \sqrt{\frac{kT_i}{2\pi M_i}} A_p e \left\{ \sqrt{\frac{2}{\pi}} \left(\frac{|e\phi_p^i|}{kT_i} + \frac{M_i w^2}{2kT_i} \right)^{\frac{1}{2}} \right\} \quad (2)$$

(Hoegy and Wharton, 1973; for probe axis perpendicular to the vehicle velocity vector in the ionospheric plasma rest frame). In the above equations A_p is the probe area, $M_{e(i)}$ and $N_{e(i)}$ are the mass and density of the electron (ion)

population, $T_{e(i)}$ is the associated temperature of an assumed Maxwellian distribution, e is the fundamental electron charge, k is Boltzmann's constant, w is the satellite velocity and $\phi_p^{e(i)}$ is the baseline voltage V_B applied to the E (I) probe and referenced to the plasma potential ($\phi_p^{e(i)} = V_B - V_\infty$).

The square of the ratio $I_e(\text{sat})/I_i(\text{sat})$ can be written

$$\left(\frac{I_e(\text{sat})}{I_i(\text{sat})} \right)^2 \equiv \left(\frac{E}{I} \right)^2 = \frac{T_e}{T_i} \frac{M_i}{M_e} \left\{ \frac{1 + |e\phi_p^e/kT_e|}{(M_i w^2/2kT_i + |e\phi_p^i/kT_i|)} \right\} \quad (3)$$

with additional manipulation (assuming $|e\phi_p^e| \gg kT_e$) resulting in

$$\left(\frac{I_e(\text{sat})}{I_i(\text{sat})} \right)^2 = \frac{M_i}{M_e} \left| \frac{\phi_p^e}{\phi_p^i} \right| \quad \frac{1}{2} M_i w^2 \ll e\phi_p^i \quad (4a)$$

$$\left(\frac{I_e(\text{sat})}{I_i(\text{sat})} \right)^2 = \frac{2 |e\phi_p^e|}{M_e w^2} \quad \frac{1}{2} M_i w^2 \gg e\phi_p^i \quad (4b)$$

$$\left(\frac{I_e(\text{sat})}{I_i(\text{sat})} \right)^2 = \frac{M_i}{M_e} \left| \frac{\phi_p^e}{\phi_p^i} \right| \left(1 + \frac{M_i w^2}{2e\phi_p^i} \right)^{-1} \quad \frac{1}{2} M_i w^2 \approx e\phi_p^i \quad (4c)$$

For laboratory and rocket-borne experiments equation (4a) would apply, whereas in the S3-4 satellite investigation equation (4c) applies. Equation (4c) is plotted in Figure 3 for two sets of bias potentials, $(|\phi_p^e|, |\phi_p^i|) = (2V, 1V)$ and $(1V, 2V)$. The results in Figure 3 show that with limitations placed on the ratio ϕ_p^e/ϕ_p^i , variations in $(I_e/I_i)^2$ can be taken as a direct measure of ion mass variations.

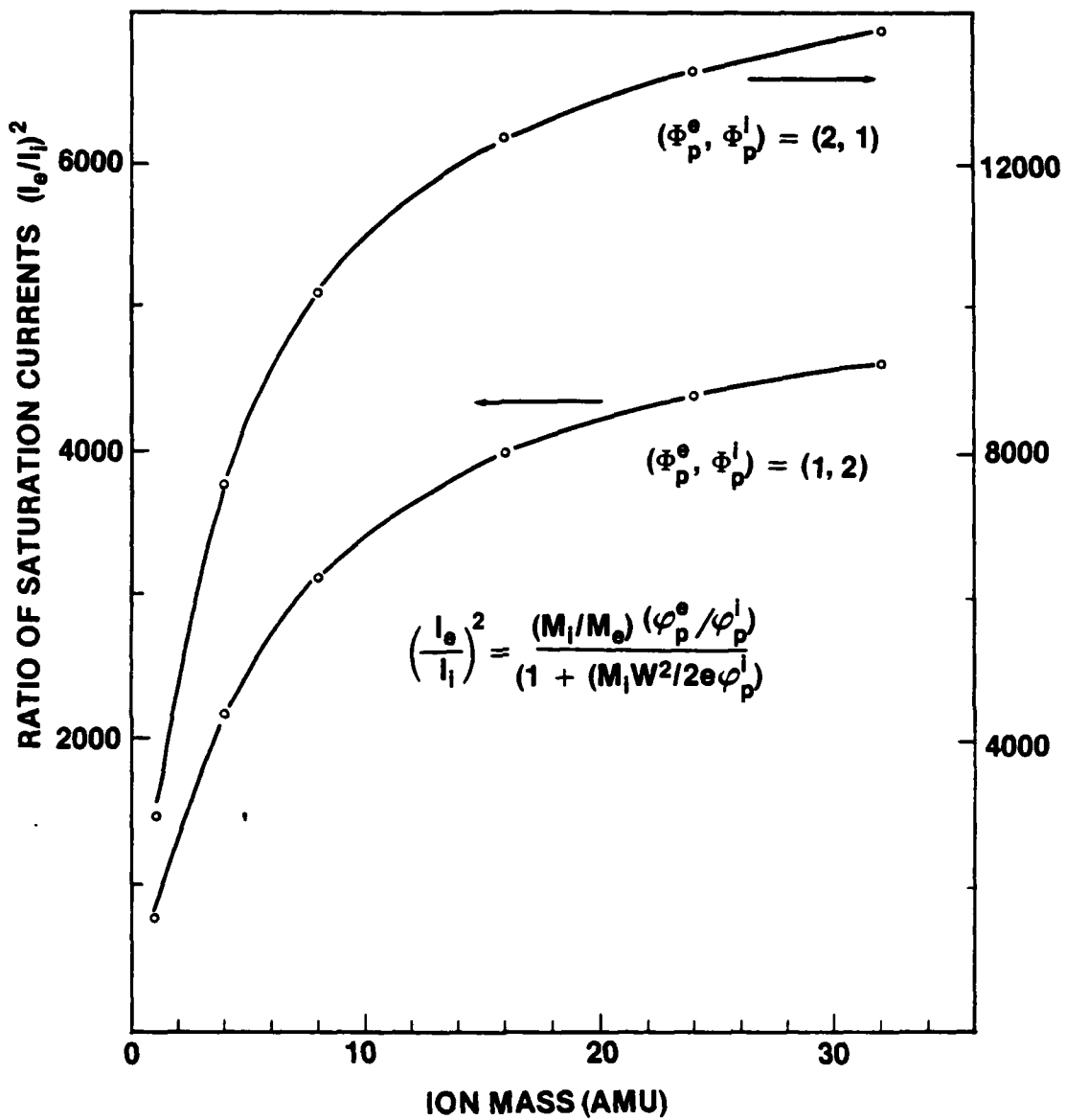


Fig. 3 — Dependence of the saturation current ratio $(I_e/I_i)^2$ on ion mass

DATA ANALYSIS AND RESULTS

Initial reduction routines for bulk processing and plotting of P⁴/S3-4 data begin with an orbit-by-orbit plot of relative electron density as measured by changes in ion- and electron-saturation currents. A representative sample of this data collected on orbit 2177 is shown in Figure 4 where the abscissa coordinates are universal time (UT), altitude (ALT in km), latitude (LAT), longitude (LONG), magnetic latitude (MLAT), and L-shell value (L). The probes' magnetic aspect angle is also plotted in the figure.

The left hand edge in Figure 4 corresponds to the satellite's ascending node (south-to-north) in the midnight hemisphere near the south magnetic pole (MLAT = -90°). With increasing time (UT) the satellite passes through the nighttime equator, the main trough, over the northern auroral oval and into the dayside ionosphere where vehicle solar cell voltage biases the entire vehicle such that both probes draw approximately equal ion saturation currents.

The simultaneous measurements of electron- and ion-saturation currents, $I_B(E)$ and $I_B(I)$ respectively, provide confidence that the observed irregularities involve plasma variations and not just secondary effects (e.g., aspect sensitivities and variations in spacecraft potential).

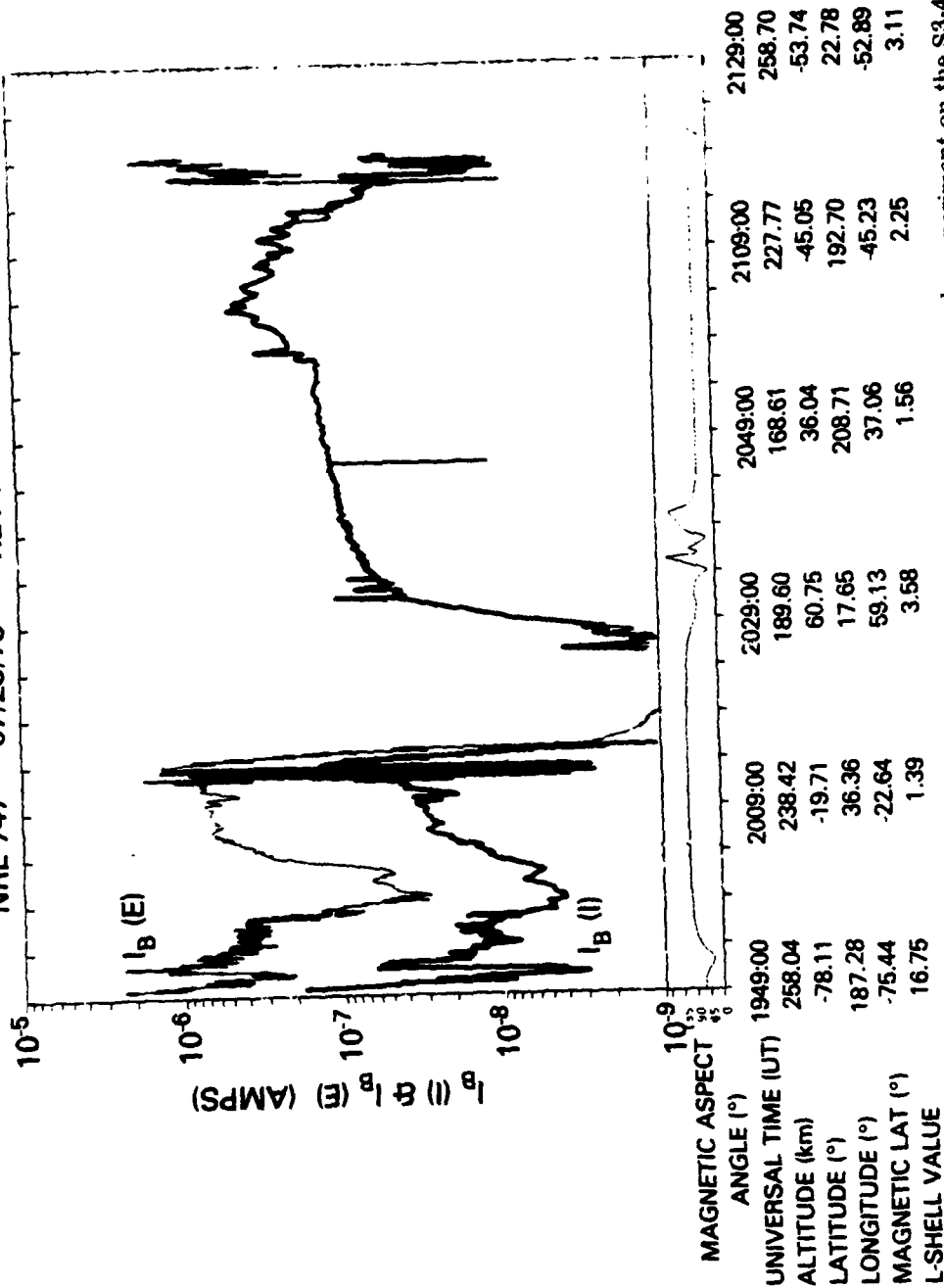


Fig. 4 — Relative electron density as measured on one complete orbit by the pulsed-plasma-probe experiment on the S3-4 satellite

Figure 4, characteristic of data accumulated to date, shows that the nighttime F-region is orders of magnitude more irregular than its dayside counterpart. The irregularities in the nighttime southern high-latitude region ($MLAT < -40^\circ$) is considered characteristic of that domain, with the most intense structures generally showing electron density variations less than an order of magnitude. There are other characteristic features in the data within $\pm 15^\circ$ of the nighttime equator, where observations of large scale plasma depletions (1 to 3 orders of magnitude) occur with a frequency typical of equatorial spread-F.

While data sets like that shown in Figure 4 provide a global map of large scale ionospheric features, primary investigative objectives are directed at the relationships between the large scale features and much smaller scale irregularities (tens of meters and less) believed to result from multistep plasma processes. To this end, the fundamental data sets $I_e(\text{sat})$ and $(I_e(\text{sat})/I_i(\text{sat}))^2$ are Fast Fourier analyzed to determine their density fluctuation power spectra, $P_N(k)$ and $P_M(k)$ respectively, where

$$\left| \frac{\delta I_e}{\bar{I}_e} \right|^2 \equiv \left| \frac{\delta N_e}{\bar{N}_e} \right|^2 \rightarrow P_N(k) \quad (5)$$

and

$$\frac{\delta(I_e/I_i)^2}{(I_e/I_i)^2} \equiv \frac{\delta \bar{M}_i}{\bar{M}_i} \rightarrow P_M(k) \quad (6)$$

The analytical relationship between $\delta N_e/\bar{N}_e$ and $\delta \bar{M}_i/\bar{M}_i$ can be simply established for a 2-component ion distribution of masses and densities (M_α, M_β) and (N_α, N_β) respectively. We do this by use of the definitions

$$\bar{M}_i = \frac{M_\alpha N_\alpha + M_\beta N_\beta}{(N_\alpha + N_\beta)} \quad (6a)$$

$$N_e = N_\alpha + N_\beta \quad (6b)$$

$$N_\alpha = N_\alpha^0 + N_\alpha^1 \quad (6c)$$

$$N_\beta = N_\beta^0 + N_\beta^1 \quad (6d)$$

$$\delta N_e = \delta N_\alpha + \delta N_\beta = N_\alpha^1 + N_\beta^1 \quad (6e)$$

and a straightforward manipulation to derive

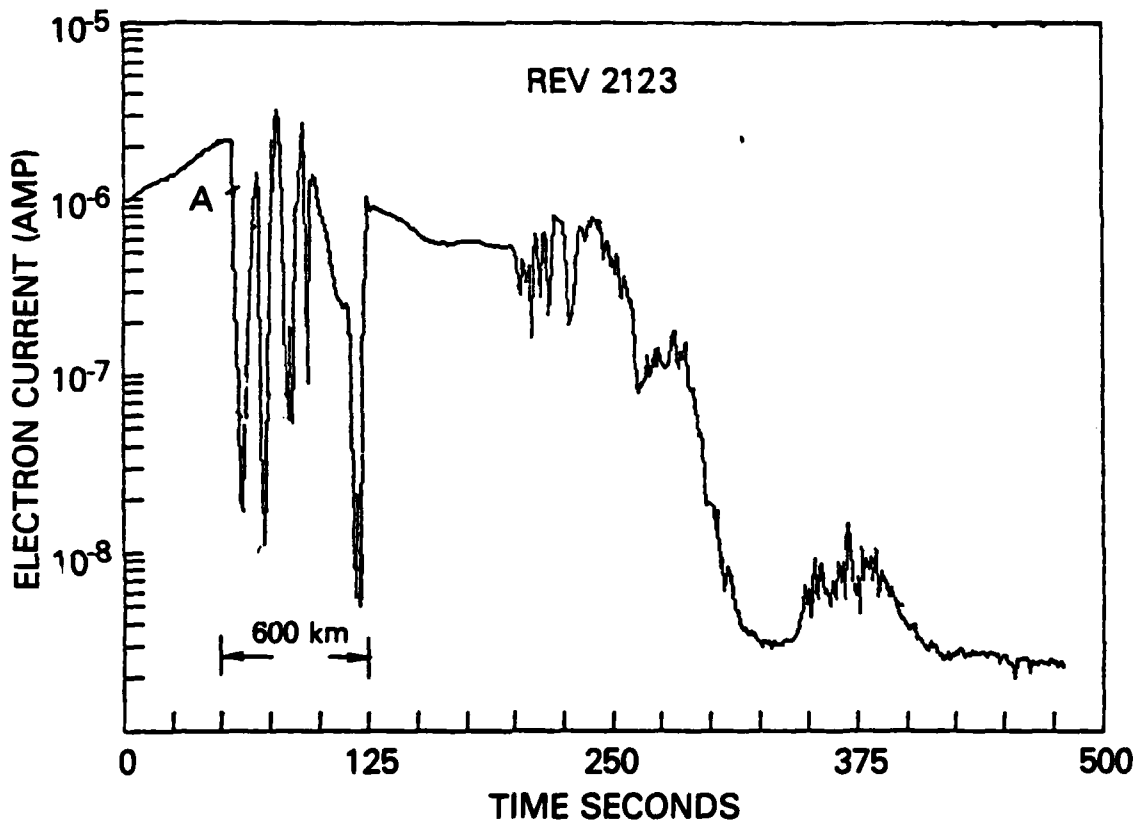
$$\frac{\delta \bar{M}_i}{\bar{M}_i} = \frac{\delta N_e}{\bar{N}_e} f(\alpha, \beta) \quad (7a)$$

where

$$f(\alpha, \beta) = \left\{ \frac{\left(\frac{M_\alpha}{M_\beta} \right) - 1}{\left(\frac{M_\alpha}{M_\beta} \right) \left(\frac{N_\alpha^0}{N_\beta^0} \right) + 1} \right\} \left\{ \frac{N_\alpha^1/N_\beta^1 - N_\alpha^0/N_\beta^0}{\left(N_\alpha^1/N_\beta^1 \right) + 1} \right\} \quad (7b)$$

It is appropriate to note that the experimental determination of mean-ion-mass fluctuations $\delta\bar{M}_i$ ($\rightarrow P_M$), through variations in $[I_e(\text{sat})/I_i(\text{sat})]^2$, assumes the relative constancy of all potentials. (This includes the spacecraft potential as well as the potentials which each probe presents to the plasma.) The spacecraft potential can vary as a direct result of changes in local plasma density since the floating potential of a body is dependent upon the ratio of its radius to the Debye length. For large space vehicles however, floating potential variations caused by even substantial plasma density variations should be small (Szuszczewicz, 1972). Another possible source of potential variations involve charging of contamination layers on the vehicle and/or on the probes (Szuszczewicz and Holmes, 1975). From the S3-4 data examined to date, variations in $(I_e/I_i)^2$ associated with charging on contamination layers, appear to be a slowly varying function of time with no attendant effects on P_M . Therefore, we have concluded that the spectral dependence of P_M is indeed representative of variations in mean-ion-mass $\delta\bar{M}_i$.

To experimentally demonstrate $P_M(k)$ and the associated relationship with $P_N(k)$ consider the high-resolution measurements (rev #2123) of the relative electron density across the nighttime equator (Figure 5). The peak electron density is approximately $5 (10^5) \text{ cm}^{-3}$ at $I_B = 3 (10^{-6})$ amp. The large scale depletions are seen to extend to 2 orders of magnitude with widths ranging from 50 to 170 km over a 600 km orbital segment.



UT 10:50:22
 ALT 241.1 km
 LAT -18.71°S
 LONG 175.9°E

10:58:42
 219 km
 11.9°N
 170.3°E

Fig. 5 — An expanded view of relative electron density encountered during the nighttime equatorial crossing on S3-4 rev 2123. The relative electron density is presented by baseline electron saturation current.

In Figure 6 are presented the P_N and P_M results for a 1 second interval located by point A in the density profile of Figure 5. Fitting the results to a power law behavior we find

$$P_N = A_n f^{-2.9} \quad (8a)$$

and $P_M = A_m f^{-1.5} \quad (8b)$

By assuming that the time (frequency) domain spectral analysis in Figure 6 can be converted to wavelength through the vehicle velocity (7.53 km/sec), the experiment shows $f_N^{-2.9}$ ($\propto k^{-2.9}$) from $k \approx 2\pi/1 \text{ km}^{-1}$ to $k = 2\pi/20 \text{ meters}^{-1}$. This is the first such satellite determination to wavelengths as short as 20 meters, with the earlier work of McClure and Hanson (1973) having defined some of the spectral features of equatorial spread-F down to 70 meters. (Conversion to the component of k perpendicular to the geomagnetic field extends the low wavelength end of Figure 6 down to $k = 2\pi/6 \text{ meter}$, the approximate value for the O^+ Larmor radius.)

The spectral index for P_N is approximately 15% steeper than previously reported values for conditions of bottomside spread-F (Keskinen et al., 1981) but well within the distribution of S3-4 spectral indices currently being accumulated and analyzed (Singh, currently unpublished) for conditions identified with the intermediate wavelength domain ($k = 2\pi/1 \text{ km}^{-1}$ to $k = 2\pi/20 \text{ m}^{-1}$).

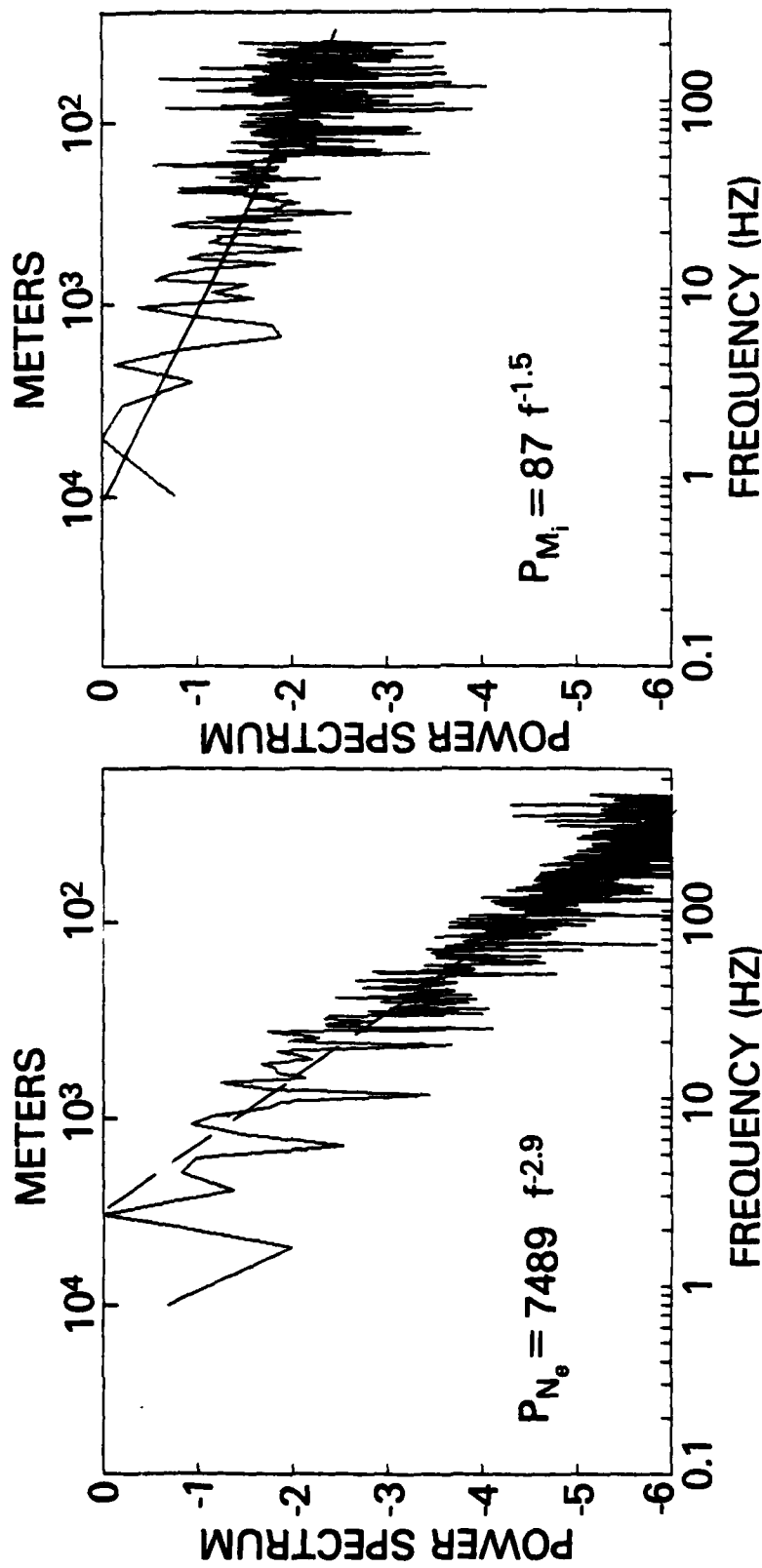


Fig. 6 — Sample illustration of simultaneously determined density fluctuation power spectrum P_N and mean ion mass fluctuation power spectrum P_M

The $P_M \propto f^{-1.5}$ observation is the first of its kind and unique to the NRL-747/S3-4 experiment. Currently there are no computational guidelines on the expected behavior, but there is sufficient evidence in laboratory plasma studies to warrant such systematic considerations of ions and their role in the hierarchy of possible mechanisms covering the spectrum of observed ionospheric irregularities. The importance of ions is clear...even from the simple considerations of the Rayleigh-Taylor instability in which a difference in charged-particle drift velocities produces an electric field across a horizontal perturbation. These drift velocities are mass dependent ($\vec{V}_i \propto M_i(\vec{g} \times \vec{B})/B^2$) and vary directly as the mass of the i^{th} species. Similar mass discriminatory effects play an important role in ambipolar diffusion processes across gradients in plasma density. The process operates more rapidly on lighter ions and can result in "patches" of varying ion mass, with local variations in conductivity and electric fields, and ultimately an ion dependent interaction in the process of energy dissipation in the large-to-small scale irregularity distribution. The P_M measurement has been designed to test for just that type of interactive mode.

$\delta\bar{M}_i/\bar{M}_i$ is a fairly complicated function of M_α/M_β , N_α^0/N_β^0 , N_α^1/N_β^1 and $\delta N_e/\bar{N}_e$ itself (See Eq. 7b); and at this point we can only speculate on the many manifestations that P_N and P_M might take for the varied ionospheric conditions encountered in the S3-4 mission. For example, it has been suggested (J.R. Goldman, private communication) that differences in gradient scale lengths for N_e and $M_{\alpha,\beta}$'s would result in a more rapid fall off with increasing k for the quantity with an initially larger gradient scale length. This difference should be a direct observable through the P_N and P_M determination. Furthermore, there is the possibility that the simultaneous measurement of $P_M(k)$ could help differentiate between a k^{-2} spectrum due to sharp edges and a k^{-2} spectrum due to gradient-drift or say drift-dissipative waves.

Currently, we have not analyzed sufficient data to exact any of the above analyses. We are at the beginning of a synoptic study designed to systematically unfold the interdependence of P_N and P_M , and the contributing roles of ion mass distributions through M_α/M_β and N_α^0/N_β^0 . However, the results in Figure 6 as well as in Figure 7 can be used to reflect some of our observations:

(i) The absolute power in P_N is generally much greater than that in P_M . In Figure 6, for example, power law fits yield $A_n/A_m \sim 86$, reflecting a situation in which the absolute density fluctuations $\delta N_e/\bar{N}_e$ are two orders of

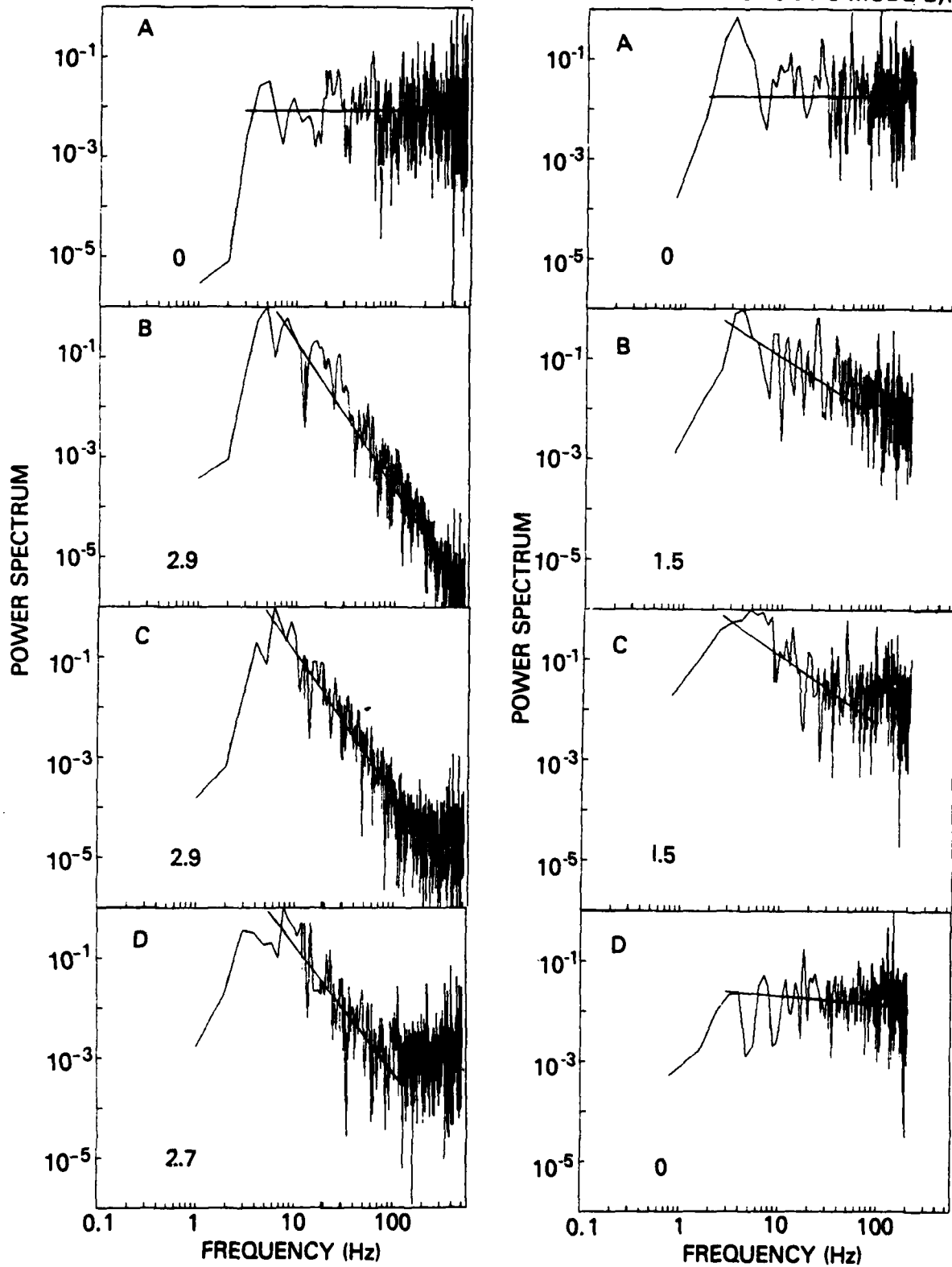


Fig. 7 - Four contiguous FFT's of electron density fluctuations (left side A through D) and simultaneously determined fluctuations in mean ion mass (right side A through D)

magnitude more intense than counterparts in $\delta\bar{M}_1/M_1$.

(ii) More often than not the k-dependence of P_N is maintained to shorter wavelength (higher frequencies) than $P_M(k)$.

(iii) The relationship between the spectral indices of P_N and P_M is highly variable. Figure 7 is an illustration of a random selection of 1.2-second interval spectra near the domain sampled in Figure 6. Panel A represents the power spectrum of the quiescent region before the depletion, while panels B through D represent contiguous power spectra within the depletion. In the quiescent region (Panel A), both density and mean ion mass fluctuations show noise spectra, while inside the depletion well-defined k-dependencies in P_N and (less frequent) k-dependent spectra in P_M are observed. While small in number, this sample of data is rather representative of results accumulated to date. More frequently than not P_M is equal to or softer than P_N (e.g., panels B,C and D). In addition, there are observations of well-defined k-spectra in P_N with none in P_M (i.e., only noise, as in panel D). Panel D is interpreted as an unstable plasma environment with a single component ion population. This is in agreement with the predictions of Eq. (7b) with $M_\alpha = M_\beta$.

Results like those outlined above are continuing with a view to a synoptic definition of the P_M, P_N interdependence and the associated roles of \bar{M}_1 , gradient scale lengths and geoplasma conditions (N_e, T_e and MLAT).

COMMENTS AND CONCLUSIONS

In order to develop a more comprehensive experimental profile on ionospheric irregularities, the pulsed plasma probe technique has been expanded to include the measurement of mean ion mass and associated mass variations, $\delta M_i / M_i$, on a spatial scale limited only by geometry and telemetry. Conducted simultaneously with the standard determinations of absolute density N_e , temperature T_e , and density fluctuation power spectra $\delta N_e / \bar{N}_e \rightarrow P_N(k)$, the expanded capability has opened up investigations which explore the coupling of electron and ion plasma wave energies which may influence the way in which large scale plasma perturbations cascade to much smaller dimensions.

Although the relationship between $\delta M_i / \bar{M}_i$ and $\delta N_e / \bar{N}_e$ is a complicated function of ratios in the ion populations, i.e., M_α / M_β , N_α^0 / N_β^0 , N_α^1 / N_β^1 , it may be systematically related to absolute densities, gradient scale lengths and time in cascading instability processes.

The new technique has been successfully flown on an F-region, polar orbiting satellite with some of the early results including:

(1) Extension of δN_e measurement capability down to dimensions of the order 5-20 meters, with associated power spectra of spectral index in the range 1.6 to 2.9. While short of the 1-3 meter limit desirable for comparison with Jicamarca or Altair radar coherent scatter results, the S3-4

experiment goes beyond the 70 meter limit of earlier satellite measurements and lends itself to additional arguments which support the association of the Rayleigh-Taylor instability occurrence of equatorial spread-F.

(2) Measurements of $\delta\bar{M}_i$ with resolution that allows detection of macroscale features (e.g., transitions from O^+ dominant to NO^+ dominant environment) and microscale spectral analysis down to dimensions comparable to the δN_e capability. As expected, power law fits ($P(k) = Af^{-X}$) to P_N and P_M have revealed considerable variations with X_M generally (but not always) smaller than X_N . Similarly, the absolute power A_M in ion mass fluctuations have been found to be considerably less (@ 2-100) than the power in P_N . A systematic study of the detailed relationships and dependence on zero-order plasma conditions is currently underway.

ACKNOWLEDGMENT

The authors wish to thank the Air Force Space Test Program, the Naval Space Systems Activity and the Office of Naval Research for support throughout this program. We are also indebted to M. G. Swinney and L. S. Kegley for their diligent efforts in all phases of fabrication, testing and integration. This work was supported within the Ionospheric and Stratospheric Task Area (09490) and conducted within the Ionospheric Diagnostics Section of the Space Science Division.

REFERENCES

- Brinton, H.C., Mayr, H.G. and Newton, G.P., "Ion composition in the nighttime equatorial F-region: Implications for chemistry and dynamics (abstract)", EOS Trans. AGU 56, 1038 (1975).
- Chen, F.F., "Electrical probes", in Plasma Diagnostic Techniques, ed. by R.H. Huddestone and S.L. Leonard (Academic, N.Y. 1965) p. 113.
- Dyson, D.L., McClure, T.P. and Hanson, W.B., "In situ measurements of spectral characteristics of F-region ionospheric irregularities", J. Geophys. Res. 79, 1497 (1974).
- Hoegy, W.R. and Wharton, L.J., "Current to a moving cylindrical electrostatic probe", J. Appl. Phys. 44, 5365 (1973).
- Holmes, J.C. and Szuszczewicz, E.P., "The versatile plasma probe", Rev. Sci. Instr. 46, 592 (1975).
- Huba, J.C., Chaturvedi, P.K., Ossakow, S.L. and Towle, D.M., "High frequency drift waves with wavelengths below the ion gyro radius in equatorial spread-F", Geophys. Res. Lett. 5, 695 (1978).
- Kelley, M.C., Pfaff, R., Baker, K.D., Ulwich, J.C., Livingston, R., Rino, C. and Tsunoda, R., "Simultaneous rocket probe and radar measurements of equatorial spread-F-transitional and short wavelength results", J. Geophys. Res. (1981, in press).
- Keskinen, M.J., Ossakow, S.L. and Chaturvedi, P.K., "Preliminary report on numerical simulations of intermediate wavelength collisional Rayleigh-Taylor instability in equatorial spread-F", J. Geophys. Res. 85, 1775 (1980).

- Keskinen, M.J., Szuszczewicz, E.P., Ossakow, S.L. and Holmes, J.C., "Nonlinear theory and experimental observations of the local collisional Rayleigh-Taylor instability in a descending equatorial spread-F ionosphere", J. Geophys. Res. 86, 5785 (1981).
- McClure, J.P. and Hanson, W.B., "A catalog of ionospheric F-region irregularity behaviour based on OGO-6 retarding potential analyzer update", J. Geophys. Res. 78, 7431 (1973).
- McClure, J.P., Hanson, W.B. and Hoffman, J.H., "Plasma bubbles and irregularities in the equatorial ionosphere", J. Geophys. Res. 82, 2650 (1977).
- Narcisi, R.S. and Szuszczewicz, E.P., "Direct measurements of electron density, temperature and ion composition in an equatorial spread-F ionosphere", J. Atm. Terr. Phys. 43, 463 (1981).
- Ossakow, S.L., "Research at NRL on theoretical and numerical simulation studies of ionospheric irregularities", NRL Memorandum Report #2907, (Oct. 1974).
- Ossakow, S.L., Zalesak, S.T., McDonald, B.E. and Chaturvedi, P.K., "Nonlinear equatorial spread-F: Dependence on altitude of the F-peak and bottomside background electron density gradient scale length", J. Geophys. Res. 84, 17 (1979).
- Rodriguez, P., Singh, M., Szuszczewicz, E.P., Walker, D.N., and Holmes, J.C., "The STP/S3-4 satellite experiment: High latitude large scale density irregularities", Proceedings of the Ionospheric Effects Symposium, (ed. by J.M. Goodman, Govt. Printing Office), (1981, in press).

- Singh, M., Szuszczewicz, E.P. and Holmes, J.C., "The STP/S3-4 satellite experiment: Equatorial F-region irregularities", Proceedings of the Ionospheric Effects Symposium, (ed. by J.M. Goodman, Govt. Printing Office), (1981, in press).
- Szczuszczewicz, E.P., "Area influences and floating potentials in Langmuir probe measurements", J. Appl. Phys., 43, 874 (1972).
- Szczuszczewicz, E.P. and Holmes, J.C., "Surface contamination of active electrodes in plasmas: Distortion of conventional Langmuir probe measurements", J. Appl. Phys. 46, 5137 (1975).
- Szczuszczewicz, E.P. and Holmes, J.C., "Observations of electron temperature gradients in mid-latitude E_s layers", J. Geophys. Res. 82, 5073 (1977).
- Szczuszczewicz, E.P., "Ionospheric holes and equatorial spread-F: Chemistry and transport", J. Geophys. Res. 83, 2665 (1978).
- Szczuszczewicz, E.P., Tsunoda, R.T., Narcisi, R. and Holmes, J.C., "Coincident radar and rocket observations of equatorial spread-F", Geophys. Res. Lett. 7, 537 (1980).
- Szczuszczewicz, E.P., Holmes, J.C. and Singh, M., "Satellite and rocket observations of equatorial spread-F irregularities: A Two-dimensional model", J. Atm. Terr. Phys., (1981, in press).

FILMED
— 8